SUPPLEMENTAL MATERIAL

Li et al., http://www.jem.org/cgi/content/full/jem.20081202/DC1

IgM^{a+b-} cells do not harbor cryptic but productive V_H7183–D_H–J_H rearrangements on the WT^b allele

To test the possibility that the presence of Eμ on the $V_HE\mu^a$ allele was in some way prohibiting surface expression of a μ-chain from the other productively rearranged *Igh*^{b} allele, we sorted IgM^{a+b-} cells (single producers) from both $V_H\Delta^a/WT^b$ and $V_HE\mu^a/WT^b$ mice and cloned V_H7183-D_H-J_H rearrangements that had taken place on the WT^b allele. In an initial experiment focusing only on $V_H\Delta^a/WT^b$ mice, four out of five V_H7183-D_H-J_H rearrangements on the WT^b allele cloned from IgM^{a+b-} cells were unproductive, whereas seven out of seven V_H7183-D_H-J_H rearrangements cloned from the same WT allele but from IgM^{a+b+} cells (double producers) were productive (unpublished data). In a second experiment involving both $V_H\Delta^a/WT^b$ and $V_HE\mu^a/WT^b$ mice, all V_H7183-D_H-J_H rearrangements on the WT^b allele cloned from IgM^{a+b-} cells (single producers) were unproductive (14 unique clones from $V_H\Delta^a/WT^b$ cells and 18 unique clones from $V_HE\mu^a/WT^b$ cells; unpublished data). Surface expression, therefore, faithfully reflects VDJ assembly status on the WT *Igh*^{b} allele, providing no support for a model of Eμ-dependent and allele-specific silencing.

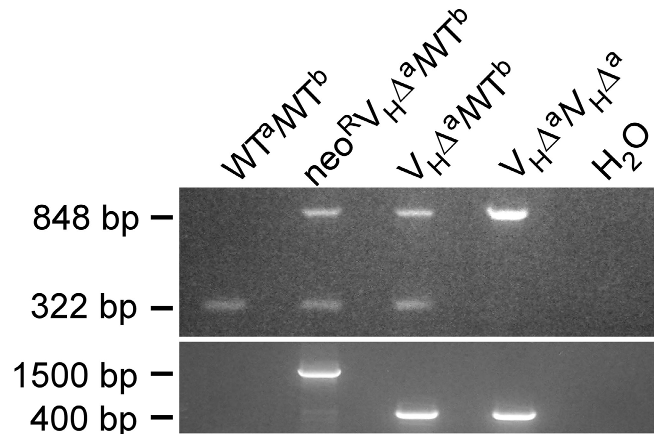

Figure S1. PCR analysis of WT and mutant F_1 mice. Top, primers generate 322-bpproduct from WT *Igh* alleles and 848-bp product from V_H knockin alleles. Bottom, primers generate ~1,500-bp product before and 400-bp product after deletion of neo^R.

Double-producers in $V_H\Delta^a/WT^b$ mice are enriched among marginal zone B cells in spleen and B1 B cells in the peritoneal cavity

As shown in Fig. 3, double producers were found in large numbers in the peritoneal cavity of $V_H\Delta^a/WT^b$ mice. Three kinds of phenotypically and functionally distinct B cell populations have been described in both mice and people: follicular B cells (also known as conventional B cells or B2 B cells), marginal zone (MZ) B cells, and B-1 B cells. Follicular and MZ B cells, as their names imply, occupy distinct regions in the spleen and can be distinguished by surface phenotype (Martin, F., and J.F. Kearney. 2002. *Nat. Rev. Immunol.* 2:323–335). Follicular B cells make up the majority of B cells in blood, lymph nodes, and spleen. The peritoneal cavity, on the other hand, is largely populated by B-1 B cells, although B-1 B cells are also found in small numbers elsewhere. B-1 B cells are subdivided into those that do (B1a) and those that do not (B1b) express CD5.

Using markers to distinguish marginal zone and follicular B cells, we examined $V_H\Delta^a/WT^b$ mice and found that the single-producers were predominantly of the follicular cell phenotype ($CD23^{hi}$, $CD21^{lo}$, IgD^{hi}, IgM^+; Supplemental Fig. 2). In contrast, the double-producers in these animals were almost equally divided between those with the follicular and those with the MZ phenotype ($CD23^{lo}$, $CD21^{hi}$, IgD^{lo}, IgM^{hi}). In the peritoneal cavity, both $V_H\Delta^a/WT^b$ and $V_HE\mu^a/WT^b$ mice had reduced numbers of cells with the B1 phenotype (relative to WT^a/WT^b mice; Fig. S2). When we analyzed the peritoneal cells for IgM^a and IgM^b, however, IgM^{a+b-} single producers were almost uniformly of the B2 phenotype ($IgD^{hi}CD5^-IgM^+B220^+$), whereas a large proportion of the double producers had a B1 phenotype (IgD^{dull} $CD5^{+/-}IgM^{hi}B220^{lo}$) (Fig. S2). In fact, among $CD5^+$ cells in the peritoneal cavity, almost all proved to be double producers.

Double producers in fetal liver and newborn spleen

To test the hypothesis that double producers were arising more frequently within progenitors to B1 B cells, fetal livers from six $V_H\Delta^a/WT^b$ embryos (day 16–18, approximately) were examined for IgM^+ cells. $B220^+$ cells were gated for analysis of the two *Igh* allotypes. As shown in Fig. S1 A, IgM^{a+b-} cells were detected in these fetal livers, but there were no obvious double producers, lending no support for the idea that B1 B cell progenitors are enriched for double producers.

To determine whether double producers dominated among the early migrants to spleen, spleen cells were isolated from newborn mice. As illustrated in Fig. S3 (and quantified in Fig. 3C), double producers in newborn spleen made up a mean of 4.4% IgM^+ cells, much as in the immature B cells of BM. Taken together, these data suggest that the large number of double producers consistently found in the spleens of $V_H\Delta^a/WT^b$ mice (~20%) results from peripheral expansion of a small pool of cells arising in the BM. The double producers found in the peritoneal cavity may similarly result from peripheral expansion of a small pool arising in fetal liver.

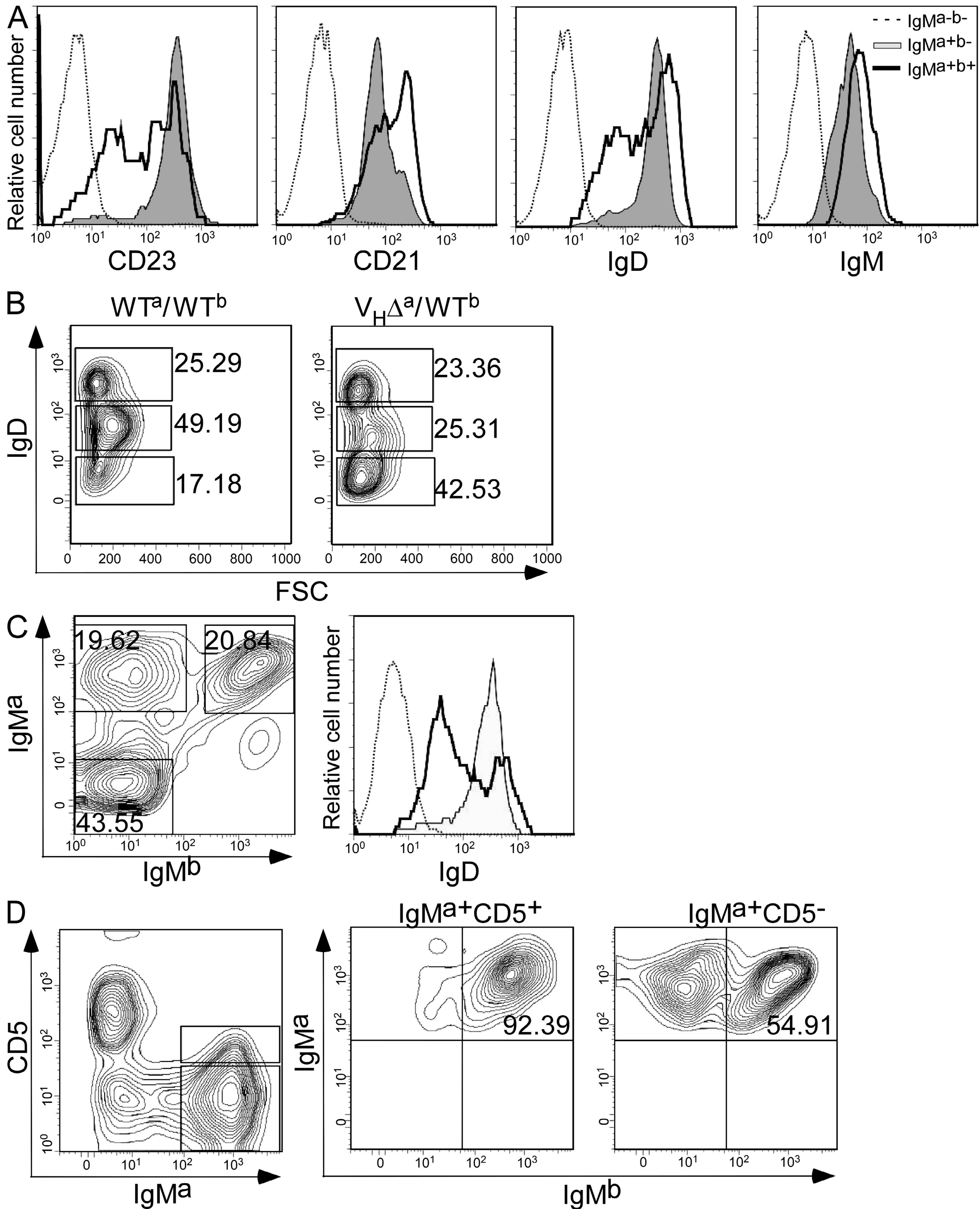

Figure S2. Surface phenotype of double-producers in spleen and peritoneal cavity of $V_H\Delta^a/WT^b$ mice. (A) CD23, CD21, IgD, and IgM expression on splenic IgM^{a+b-} cells (single producers; shaded curve) and IgM^{a+b+} cells (double producers; dark line). Non-B cells were included as controls (IgM^{a-b-}; dotted line). Cells were gated on the basis of IgM^a and IgM^b expression and histograms generated for expression of the third surface marker. (B) IgD expression on peritoneal cells (plotted versus forward scatter [FSC]). Percentage of total cells in three IgD gates (negative, dull, high) provided. (C) IgD levels on peritoneal cells gated as IgM^{a-b-}, IgM^{a+b-}, and IgM^{a+b+}. Left, contour plot of anti-IgM^a and anti-IgM^b staining, with gates and percentage of total cells indicated. Right, histogram of IgD levels on gated populations as in A. (D) IgM allotype expression on peritoneal cells. Cells were stained with antibodies to CD5, IgM^a, and IgM^b. Cells gated on the basis of CD5 and IgM^a expression (left) were analyzed for IgM^a and IgM^b expression (middle and right).

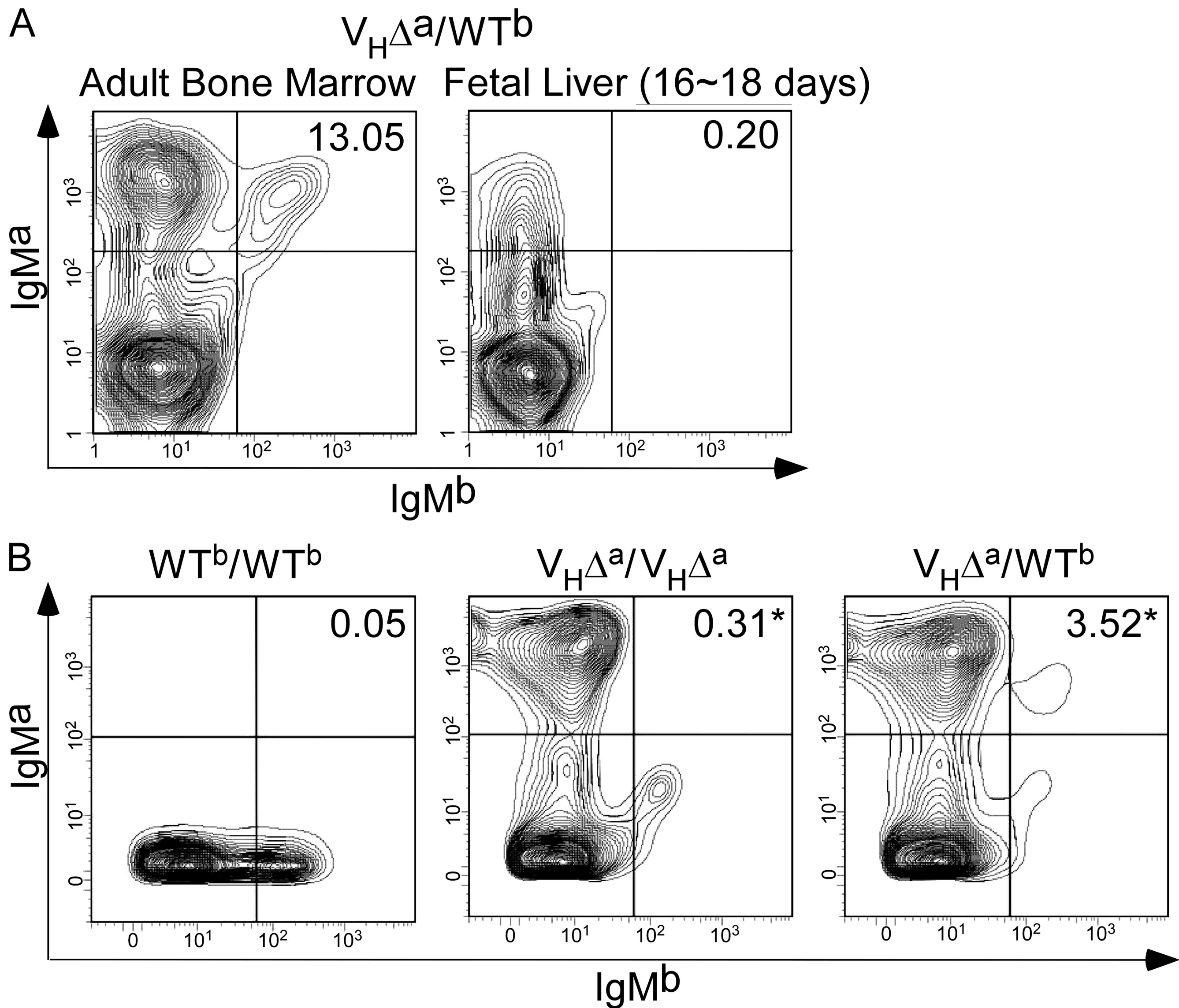

Figure S3. Ontogeny of double-producers in heterozygous $V_H\Delta^a$/WT^b mice. (A) IgM allotype expression in adult BM and fetal liver of $V_H\Delta^a$/WT^b mice. Lymphocytes isolated from one adult BM or pooled from six fetal livers (∼16–18-d embryos) were stained with FITC-conjugated anti–mouse IgM^b, PE-conjugated anti–mouse IgM^a, and APC-conjugated anti–mouse B220. Plots shown are gated for $B220^+$ cells. Numbers shown are IgM^{a+b+}/IgM cells × 100. (B) IgM allotype expression in splenic lymphocytes of a newborn C57BL/6 (WT^b/WT^b) mouse, a $V_H\Delta^a$/$V_H\Delta^a$ homozygous mouse, and a $V_H\Delta^a$/WT^b heterozygous mouse (representative of two mice analyzed). Spleen cells from ∼2–3-d-old newborn mice were stained with FITC-conjugated anti–mouse IgM^b and PE-conjugated anti–mouse IgM^a. Numbers shown are IgM^{a+b+}/IgM cells × 100. *, In these cases, the number shown is IgM^{a+b+}/(IgM^{a+b-} + IgM^{a+b+}) × 100 because the signals in the bottom right quadrant are a result of background staining that is present in mice that lack *Igh*^{b} allele (middle).

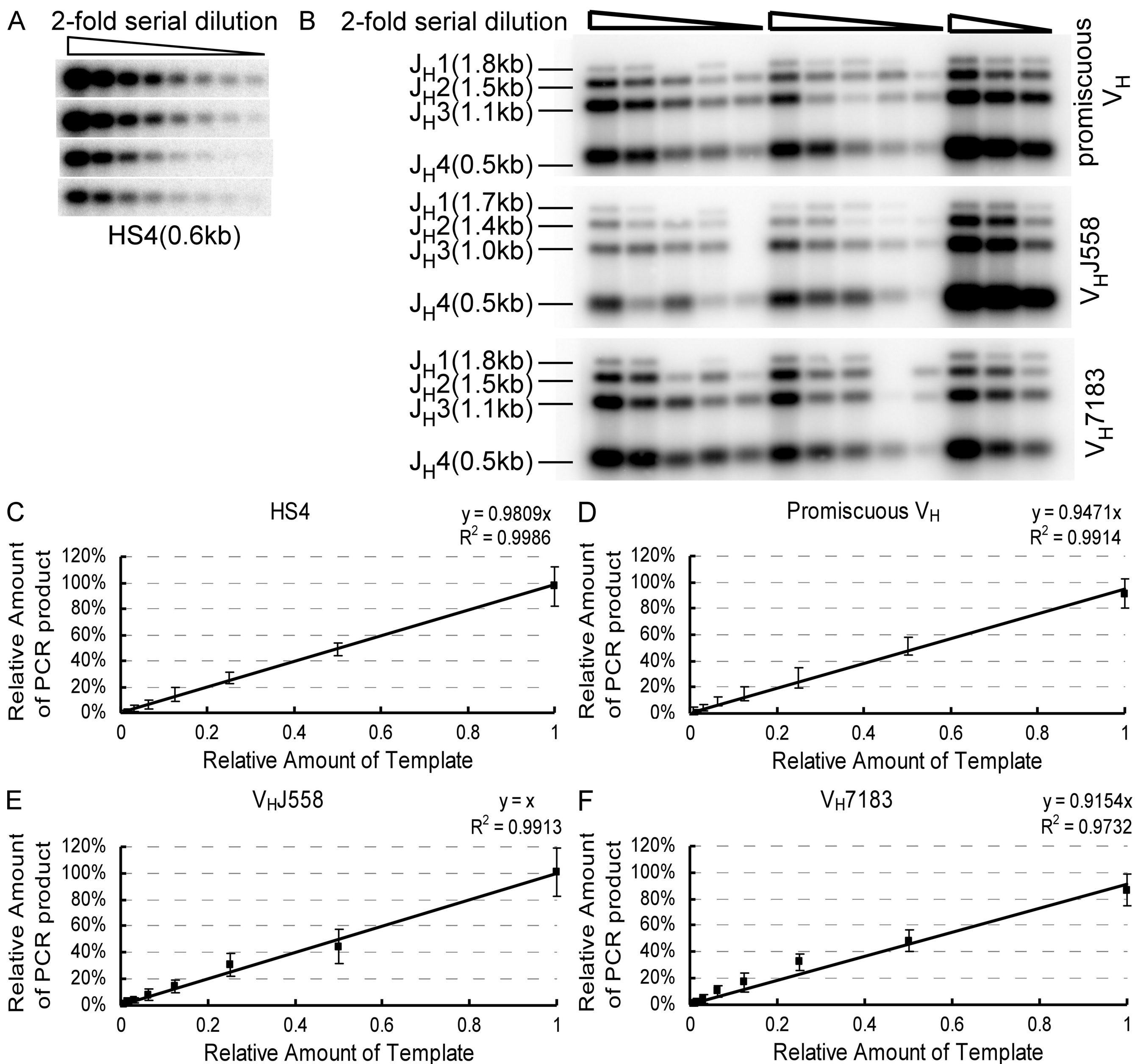

Figure S4. Quantitative analysis of V–DJ rearrangements. (A) Representative blot of HS4 PCR products using twofold serially diluted DNA samples. Dilutions of four independent samples are shown. PCRs were carried out as described in Materials and methods except that the 30-cycle PCR was reduced to 20 cycles. (B) Representative blots of VDJ PCR products using two-fold serially diluted DNA samples as template. Methods were as described in Fig. 5B. Dilutions of three independent samples are shown. (C) Quantitative analysis (ImageQuant) of HS4 blots like that shown in A. Dilutions of a total of eight independent samples were included in these analyses. For each set of twofold serially diluted samples, the amount of template in the first sample was assigned a value of 1, the second a value of ½, the third ¼, and so on. Relative amount of PCR product for each dilution point in a series was calculated as follows: sum of template amount used in the dilution series (e.g., 1 + ½ + ¼ for a series of three dilutions) × (ImageQuant reading of the PCR product for the sample in question)/ (ImageQuant reading of the sum of the products in the dilution series). The graph is the best-fit line for data collected from eight sets of twofold serially diluted samples (Microsoft Excel trendline). (D–F) Quantitative analysis (ImageQuant) was performed as described in C for VDJ rearrangements using the promiscuous V_H primer (D), the V_HJ558 family primer (E), and the V_H7183 family primer (F). D–F are each plots of data collected from 14 independent twofold serial dilutions. Error bars show SD.

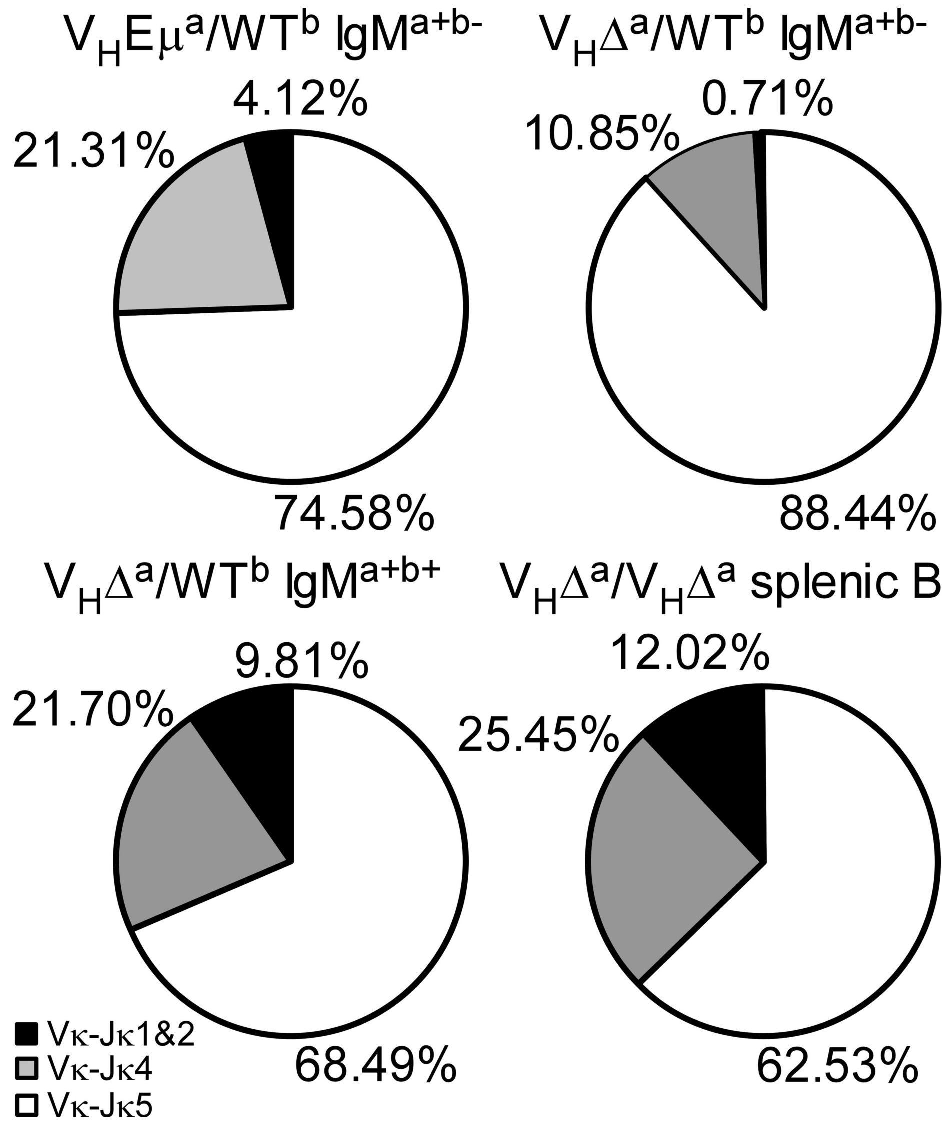

Figure S5. Pie charts showing relative usage of Jκ gene segments in splenic B cells from WT and mutant mice. Each PCR product was quantified (e.g., Vκ-Jκ4 products) and proportion for each PCR product was assigned relative to the summed value for all of the products (e.g., Vκ-Jκ4/(Vκ-Jκ1 + Vκ-Jκ2 + Vκ-Jκ4 + Vκ-Jκ5). Vκ-Jκ1 and Vκ-Jκ2 PCR product values were pooled for these analyses.

Table S1. Absolute cell numbers in WT and mutant mice

	Igh^b(n = 3)	$V_HE\mu^a/V_HE\mu^a$(n = 3)	$V_H\Delta^a/V_H\Delta^a$(n = 3)
BM (× 10^6)			
Total cells	25.83 ± 2.84	21.83 ± 6.45	21.50 ± 1.00
Lymphocytes	7.22 ± 0.24	4.94 ± 1.17	5.10 ± 0.56
B220$^+$	4.20 ± 0.12	1.84 ± 0.44*	2.22 ± 0.37*
Pro-B	0.49 ± 0.07	0.27 ± 0.06*	0.35 ± 0.10
Pre-B	2.09 ± 0.26	0.78 ± 0.17*	0.88 ± 0.31*
Immature B	0.44 ± 0.05	0.21 ± 0.07*	0.19 ± 0.07*
Mature B	0.88 ± 0.13	0.40 ± 0.14*	0.53 ± 0.20*
Spleen (× 10^6)			
Total cells	33.00 ± 2.18	31.67 ± 4.80	36.50 ± 5.07
Lymphocytes	26.85 ± 2.88	25.46 ± 4.09	29.59 ± 3.59
B cells	14.36 ± 2.68	12.97 ± 2.32	14.60 ± 0.40
T cells	9.28 ± 0.67	9.61 ± 1.35	11.16 ± 1.95

Cells recovered from BM and spleen of individual mice were counted (total cells). Aliquots were stained for B-lineage markers (B220, CD43, IgD, and IgM in BM) and for CD3-ε (T cells) and B220 (B cells) in spleen. Cell number for lymphocyte subpopulations were calculated based on total cell count and the percentage of total cells comprising each subpopulation (determined by flow cytometry). *, P < 0.001 (vs. *Igh*^{b}/*Igh*^{b}) by two-tailed Student's t-test. *n* = number of animals.

Table S2. V_H-D_H-J_{H4} junction sequences on the WT *Igh*^{b} allele of $V_H\Delta^a$/WT^b and $V_HE\mu^a$/WT^b pre-B cells.

$V_HE\mu$ ^{a}/WT^b pre-B cells V_H7183-D_H-J_H4 rearrangements

V name	3'V-REGION	N1	P	D-REGION	N2	D name	Productivity	CDR3 length
IGHV5-2	tgtgcaaga	ctt		ctacg	tgc		P	12
IGHV5-2	tgtgcaaga	c		atagtaaccac	ttgacg	IGHD3-1	P	12
IGHV5-2	tgtgcaaga	cat		gtctatgc	cacgggggg		P	14
IGHV5-2	tgtgcaaga	caag		taactggg		IGHD4-1	P	10
IGHV5-2	tgt	ccc		tggtt		IGHD2-3	P	8
IGHV5-2	tgtgcaaga	ca		taactggg		IGHD4-1	P	11
IGHV5-2	tgtgcaaga	ctt		ctacg	tgc		P	12
IGHV5-2	tgtgcaaga	c		actacggtagtagc		IGHD1-1	NP	
IGHV5-2	tgtgcaaga	cgactg		ggtggt			NP	
IGHV5-2	tgtgcaaga			tggttactac	a	IGHD2-3	NP	
IGHV5-2	tgtgcaaggac			ctcccgcta	t		NP	
IGHV5-2	tgtgcaaga	c		atagtaactac	aacgagct	IGHD3-1	NP	
IGHV5-2	tgtgcaaga	c		atagtaactac	gacgagct	IGHD3-1	NP	
IGHV5-2	tgtgc			tactata	t	IGHD3-1	NP	
IGHV5-2	tgtgcaaga			tggttacga	gagagggggggggt	IGHD2-7	NP	
IGHV5-2	tgtgcaaga	c		tagtaactac	gtat	IGHD3-1	NP	
IGHV5-2	tgtgcaaga	catgggc		ccaaataggg	g		NP	
IGHV5-2	tgtgcaaga	c		atgg	gg		NP	
IGHV5-2	tgtgcaaga	c		actatagtaact	ggggg	IGHD3-1	NP	
IGHV5-2	tgtgcaaga	c		atagtaactac	gacgagct	IGHD3-1	NP	
IGHV5-2	tgtgcaaga			ctactatagtaac	cctgt	IGHD3-1	NP	
IGHV5-4	tgtgcaaga	ga		tctccgggggtg	gtct		P	13
IGHV5-4	tgtgcaaga	g		atggtaactac	gt	IGHD2-8	P	13
IGHV5-4	tgtgcaaga			gtac			NP	
IGHV5-4	tgtgcaag			ctactatagtaac	ga	IGHD3-1	NP	
IGHV5-4	tgtgcaaga	gat		ctatgattacgac	gacggcccc	IGHD2-4	NP	
IGHV5-4	tgtgcaaga	gagagttct	t	agacagctcagg	gacggg	IGHD3-2	NP	
IGHV5-4	tgtgcaaga	gatgg		ggtagtagc	aatctc	IGHD1-1	NP	
IGHV5-6	tgtgcaagaca			taagacg	a		P	12
IGHV5-6	tgtgcaagaca			ttattactacg	agggctac	IGHD1-1	P	11
IGHV5-6	tgtgcaagac	cg		gggaggttcta	g		NP	
IGHV5-12	tgtgcaaga	catg		actatgactacgac	ggttgg	IGHD2-4	P	15
IGHV5-12	tgtgcaaga	c		atgtctatgac	cccct	IGHD2-3	P	14
IGHV5-12	tgtgcaaga	catcctc		atggttactac	gtcc	IGHD2-3	NP	
IGHV5-9-1*	(Cys 114 is missing)						NP	
IGHV5-17	tgtgcaagg	Cgaatcagccag		attactacggtagtag	ggaag	IGHD1-1	P	17
IGHV5-17	tgtgcaagg	aggaacggg		actacggtagtag	aag	IGHD1-1	P	15

$V_H\Delta$ ^{a}/WT^b pre-B cells V_H7183-D_H-J_H4 rearrangements

V name	3'V-REGION	N1	P	D-REGION	N2	D name	Productivity	CDR3 length
IGHV5-1	tgtttgaga	cat		cctact	tt		NP	
IGHV5-1	tgtttgaga	c		tggtaac		IGHD2-8	NP	
IGHV5-2	tgtgcaag	cat		cttcgg			P	7
IGHV5-2	tgtgcaaga			catcgggg	cccc		P	12
IGHV5-2	tgtgcaaga	gaccg					P	9
IGHV5-2	tgtgcaag	cat		cttcgg			P	7
IGHV5-2	tgtgcaaga	cat		tactatgattacgac	ggg	IGHD2-4	P	14
IGHV5-2	tgtgcaaga	cat		gacagctcaggctac	ac	IGHD3-2	NP	
IGHV5-2	tgtgcaaga	ca		ggggcagctcaggc	cct	IGHD3-2	NP	
IGHV5-2	tgtgcaaga			tgattacga		IGHD2-4	NP	
IGHV5-2	tgtgcaag	g		ctgaagt	agga		NP	
IGHV5-2	tgcgcaaga			tctactatgattacgac	gggg	IGHD2-4	NP	
IGHV5-2	tgtgcaaga			cctactatag		IGHD3-1	NP	
IGHV5-2	tgtgcaaga	c		tagc			NP	
IGHV5-2	tgtgcaaga	catgg		atagtaactac	ggaagg	IGHD3-1	NP	
IGHV5-2	tgtgcaaga	ct		gtaactac	g	IGHD3-1	NP	
IGHV5-2	tgtgcaaga	caagtaa		aaagggg	cttg		NP	
IGHV5-2	tgtgcaaga			ctatgattacgac	ggga	IGHD2-4	NP	
IGHV5-2	tgtgcaaga	tttcccсttg		ggtaactac	g	IGHD2-8	NP	
IGHV5-2	tgtgcaaga	c		atggtaactac	g	IGHD2-8	NP	
IGHV5-2	tttgcaaga			tgattacga		IGHD2-4	NP	
IGHV5-2	tgtgcaaga	cgga		ggtagtagctac	gggg	IGHD1-1	NP	
IGHV5-4	tgtgcaaga	gatc		acgatagtaactac	g	IGHD3-1	P	14
IGHV5-4	tgtgcaaga	gataact	a	tctactatggttacga	gcgacccct	IGHD2-7	NP	
IGHV5-4	cgtgcaaga	gaa		ggaatggtaagg		IGHD2-8	NP	
IGHV5-4	tgtgcaaga			gatagcccagg	gacgggg	IGHD3-2	NP	
IGHV5-6	tgtgcaag	ccctcg	a	tttattactacgg	tagtagct	IGHD2-3	NP	
IGHV5-9	tgtgcaaga			tctatgatggttactac	g	IGHD2-3	P	14
IGHV5-9	tgtgcaag	gc		ataa	g		P	8
IGHV5-9	tgtgcaaga	t		ggtaacacgg		IGHD2-8	NP	
IGHV5-9-1	tgtacaaga			gagggttact		IGHD2-3	P	12
IGHV5-9-1	tgtacaaga	gacgggggcct		gggacag	g	IGHD4-1	P	14
IGHV5-9-1	tgtacaaga	gaggagatgg		taccctcaata			NP	
IGHV5-16	tgtgcaaga	gatcaga		atgattacgac	ggg	IGHD2-4	P	14
IGHV5-17	tgtgcaagg	ccc		acgggg			NP	
IGHV7-3**	tgtgcaagatat	ctg		aactggg	ctagg	IGHD4-1	P	12

V_H7183$D_H$$J_{H4}$ rearrangements were cloned by PCR from genomic DNA of isolated pre-B cells using a V_H7183 family primer and J_{H4} primer. DNA sequences were analyzed by the IMGT/V-QUEST program (http://imgt.cines.fr). Because of ambiguity, assigned D_H genes were manually revised where necessary, using IMGT/V-QUEST results as guidance, and junctions without a perfect alignment of seven or more nucleotides to a C57BL/6 D_H gene were not assigned a D_H gene. P, productive; NP, non-productive. CDR3 lengths were given for productive clones (the IMGT/V-QUEST program assigns the CDR3 to sequences between Cys 104 in the V_H and Trp/Phe in the conserved Trp/Phe-Gly-X-Gly motif in J_H). Clones were isolated in two separate experiments: in one experiment, clones were obtained from pre-B cells of an individual $V_HE\mu^a$/WT^b and an individual $V_H\Delta^a$/WT^b mouse; in the second experiment, pre-B cells were isolated from a pool of two mice for each genotype. *, in this rearrangement, the V_H and J_H genes can be identified, but the Cys 104 was missing so the junction was not analyzed. **, the V_H used in this rearrangement is from another (non 7183) V_H family.